SIAM J. SCI. STAT. COMPUT.
Vol. 11, No. 2, pp. 389–397, March 1990

011

A NOTE ON THE USE OF SYMMETRIC LINE GAUSS–SEIDEL FOR THE STEADY UPWIND DIFFERENCED EULER EQUATIONS*

WIM A. MULDER†

Abstract. Symmetric Line Gauss–Seidel (SLGS) relaxation, when used to compute steady solutions to the upwind differenced Euler equations of gas dynamics, is shown to be unstable. The instability occurs for the long waves. If SLGS is used in a multigrid scheme, stability is restored. However, the use of an unstable relaxation scheme will not provide a robust multigrid code. Damped Symmetric Point Gauss–Seidel relaxation is stable and provides similar multigrid convergence rates at much lower cost. However, it fails if the flow is aligned with the grid over a substantial part of the computational domain. Damped Alternating Direction Line Jacobi relaxation can overcome this problem.

Key words. line relaxation, stability, multigrid method, steady Euler equations

AMS(MOS) subject classifications. 35L65, 65N20, 76N15

1. Introduction.

The Euler equations that describe the flow of an inviscid compressible gas can be integrated in time by means of an implicit method. This is desired if the flow displays features on different scales, or if the steady state has to be computed efficiently. The implicit formulation gives rise to a large sparse system of linear equations, which can be solved by factorization methods such as the Alternating Direction Implicit method [4] and Approximate Factorization [1]. However, if the spatial discretization is obtained by upwind differencing, the implicit system is diagonally dominant and can be solved more efficiently by classical relaxation methods. This was pointed out and explored by van Leer and myself [15], and, independently, by Chakravarthy [3].

In [15] we found that one particular relaxation method, Symmetric Line Gauss–Seidel (SLGS), did not converge as fast as expected, and sometimes did not converge at all. This was thought to be caused by the numerical boundary conditions. The same problem was encountered in [13].

Here it is shown that the convergence problem is due to the intrinsic instability of the SLGS scheme. In §2, the classical von Neumann stability analysis is carried out on the system of linearized Euler equations in two dimensions. As the Fourier modes used in the analysis are not the proper eigenfunctions for Gauss–Seidel relaxation, some numerical experiments were carried out with the nonlinear equations (§3).

The instability occurs for the long waves. If SLGS is applied as a relaxation scheme in a multigrid code, the corrections from coarser grids are sufficient to suppress the instability. This is shown in §4. A multigrid scheme based on SLGS relaxation has already been used in [8]. However, damped Symmetric Point Gauss–Seidel (SGS) provides similar convergence rates at a lower cost, and damped Alternating Direction Line Jacobi has much better convergence factors.

The main results are summarized in §5.

*Received by the editors August 29, 1988; accepted for publication (in revised form) March 27, 1989. This work was supported by the Center for Large Scale Scientific Computing (CLaSSiC) Project at Stanford University, under Office of Naval Research contract N00014-82-K-0335.

†Department of Computer Science, Stanford University, Stanford, California 94305-2140. Present address, Koninklijke/Shell Exploratie en Produktie Laboratorium, Postbus 60, 2280 AB Rijswijk, the Netherlands.

2. Stability analysis. The flow of an ideal inviscid compressible gas can be described by the Euler equations. In conservation form, these are given by

$$\frac{\partial w}{\partial t} + \frac{\partial f}{\partial x} + \frac{\partial g}{\partial y} = 0. \tag{2.1a}$$

The vector of states w and the fluxes f and g are

$$w = \begin{pmatrix} \rho \\ \rho u \\ \rho v \\ \rho E \end{pmatrix}, \quad f = \begin{pmatrix} \rho u \\ \rho u^2 + p \\ \rho uv \\ \rho uH \end{pmatrix}, \quad g = \begin{pmatrix} \rho v \\ \rho uv \\ \rho v^2 + p \\ \rho vH \end{pmatrix}. \tag{2.1b}$$

The density of the gas is denoted by ρ. The x- and y-component of the velocity are u and v, respectively. The energy E, total enthalpy H, pressure p, and sound speed c are related by

$$E = \frac{1}{(\gamma-1)}\frac{p}{\rho} + \frac{1}{2}(u^2+v^2), \qquad H = E + \frac{p}{\rho}, \qquad c^2 = \gamma\frac{p}{\rho}. \tag{2.2}$$

A nonconservative form of (2.1) is

$$\frac{\partial w'}{\partial t} + A\frac{\partial w'}{\partial x} + B\frac{\partial w'}{\partial y} = 0, \tag{2.3a}$$

where

$$A = \begin{pmatrix} u & 0 & c & 0 \\ 0 & u & 0 & 0 \\ c & 0 & u & 0 \\ 0 & 0 & 0 & u \end{pmatrix}, \quad B = \begin{pmatrix} v & 0 & 0 & 0 \\ 0 & v & c & 0 \\ 0 & c & v & 0 \\ 0 & 0 & 0 & v \end{pmatrix}, \quad \delta w' = \begin{pmatrix} \delta u \\ \delta v \\ \delta p/(\rho c) \\ \delta S \end{pmatrix}. \tag{2.3b}$$

Here $S = \log(p/\rho^\gamma)$ is the specific entropy.

The stability analysis will be carried out for the discretization of the linear residual operator

$$L = A\frac{\partial}{\partial x} + B\frac{\partial}{\partial y}, \tag{2.4}$$

with constant coefficients and periodic boundary conditions. The operator is discretized in space by upwind differencing. This is accomplished as follows. The matrix A is diagonalized by Q_1, according to

$$A = Q_1 \Lambda_1 Q_1^{-1}, \quad \Lambda_1 = \begin{pmatrix} u-c & & & \bigcirc \\ & u & & \\ & & u & \\ \bigcirc & & & u+c \end{pmatrix}, \quad Q_1 = \begin{pmatrix} 1 & 0 & 0 & 1 \\ 0 & -1 & 0 & 0 \\ -1 & 0 & 0 & 1 \\ 0 & 0 & 1 & 0 \end{pmatrix}. \tag{2.5a}$$

For B we have

$$B = Q_2 \Lambda_2 Q_2^{-1}, \quad \Lambda_2 = \begin{pmatrix} v-c & & & \bigcirc \\ & v & & \\ & & v & \\ \bigcirc & & & v+c \end{pmatrix}, \quad Q_2 = \begin{pmatrix} 0 & 1 & 0 & 0 \\ 1 & 0 & 0 & 1 \\ -1 & 0 & 0 & 1 \\ 0 & 0 & 1 & 0 \end{pmatrix}. \tag{2.5b}$$

To obtain an upwind scheme, the matrix Λ_k ($k = 1, 2$) is split into Λ_k^+ and Λ_k^-, which contain the positive and negative elements of Λ_k, respectively. This implies

(2.6) $$\Lambda_k^+ + \Lambda_k^- = \Lambda_k, \qquad \Lambda_k^+ - \Lambda_k^- = |\Lambda_k|.$$

Now define

(2.7) $$A^\pm \equiv Q_1 \Lambda_1^\pm Q_1^{-1}, \qquad B^\pm \equiv Q_2 \Lambda_2^\pm Q_2^{-1}.$$

It follows that

(2.8) $$\begin{aligned} A &= A^+ + A^-, \qquad |A| \equiv Q_1|\Lambda_1|Q_1^{-1} = A^+ - A^-;\\ B &= B^+ + B^-, \qquad |B| \equiv Q_2|\Lambda_2|Q_2^{-1} = B^+ - B^-. \end{aligned}$$

The discrete linear residual operator becomes

(2.9) $$L^h \equiv \frac{1}{h_x}[A^+(1 - T_x^{-1}) + A^-(T_x - 1)] + \frac{1}{h_y}[B^+(1 - T_y^{-1}) + B^-(T_y - 1)].$$

Here the shift operators are defined by $T_x w_{k_1,k_2} \equiv w_{k_1+1,k_2}$, $T_y w_{k_1,k_2} \equiv w_{k_1,k_2+1}$. For simplicity, the grid is assumed to be uniform ($h_x = h_y = h$).

For the stability analysis we consider the usual Fourier modes of the form

(2.10a) $$\exp\left[-i\left(k_1\theta_x + k_2\theta_y\right)\right],$$

where k_1 and k_2 are spatial indices on a $N_1 \times N_2$ grid. The frequencies for a grid of the same size are

(2.10b) $$\theta_x = 2\pi\frac{l_1}{N_1}, \quad \theta_y = 2\pi\frac{l_2}{N_2}, \quad l_1 = 0, \cdots, N_1 - 1, \quad l_2 = 0, \cdots, N_2 - 1.$$

The Fourier transforms of the shift-operators T_x and T_y are

(2.11) $$\hat{T}_x \equiv \exp(i\theta_x), \quad \hat{T}_y \equiv \exp(i\theta_y), \quad 0 \le \theta_x < 2\pi, \quad 0 \le \theta_y < 2\pi.$$

The relaxation operator for SLGS, with the line in the y-direction, is the product of a forward sweep

(2.12a) $$\hat{G}_1 = I - \hat{M}_1^{-1}\hat{L}^h, \qquad \hat{M}_1 = \hat{L}^h - \frac{1}{h}A^-\hat{T}_x,$$

and a backward sweep

(2.12b) $$\hat{G}_2 = I - \hat{M}_2^{-1}\hat{L}^h, \qquad \hat{M}_2 = \hat{L}^h + \frac{1}{h}A^+\hat{T}_x^{-1},$$

resulting in

(2.12c) $$\hat{G}^{\mathrm{SLGS}} = \hat{G}_2\hat{G}_1.$$

Here I denotes a 4×4 identity matrix. If $\hat{M}_1$ or $\hat{M}_2$ is singular, the pseudo-inverse should be used. If these matrices are nonsingular, then we obtain

(2.12d) $$\hat{G}^{\mathrm{SLGS}} = \hat{M}_2^{-1}A^+\hat{M}_1^{-1}A^-.$$

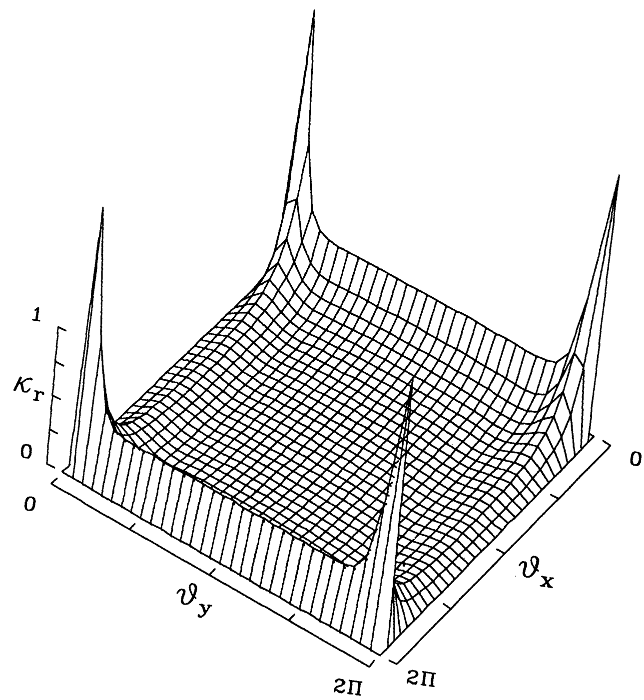

FIG. 1. *Amplification factor of* SLGS *relaxation for* $u/c = 0.8$ *and* $v/c = 0$. *The figure corresponds to a* 32×32 *grid.*

This shows that SLGS is an exact solver if $|u| \geq c$, because either A^+ or A^- vanishes in that case. The fourth equation of (2.3), which describes the convection of entropy along streamlines, is also solved exactly, for all u and v.

The stability of this scheme is investigated by computing the amplification factor of the residual

$$\text{(2.13)} \qquad \overline{\kappa}_r \equiv \max_{\theta_x, \theta_y} \kappa_r(\theta_x, \theta_y), \qquad \kappa_r(\theta_x, \theta_y) \equiv \rho\Big(\hat{L}^h \hat{G}^{\mathrm{SLGS}} (\hat{L}^h)^\dagger\Big).$$

Here $\rho(\cdot)$ denotes the spectral radius. The operator $\hat{L}^h$ can be singular [9, Lem. 3.1], and the waves for which it is singular are obviously not damped or amplified. To exclude these waves, the operator $\hat{L}^h$ and its pseudo-inverse are included in the definition of κ_r. The value of $\overline{\kappa}_r$ will depend on the velocities u/c and v/c, and on the grid-size $N_1 \times N_2$.

Figure 1 shows $\kappa_r(\theta_x, \theta_y)$ for $u/c = 0.8$ and $v/c = 0$. Here $N_1 = N_2 = 32$. The instability is clearly visible. It occurs for the long waves, at $|\theta_x| = |\theta_y| = 2\pi/32$. For the given u/c and v/c, the instability does not show up on a 16×16 grid, whereas it becomes worse on finer grids.

Similar instabilities occur for most values of $|u/c| < 1$ and $|v/c| \leq 1$, in some cases on grids coarser than in the example of Fig. 1.

3. Numerical experiments. It is well known that Fourier modes are not the proper eigenfunctions for Gauss–Seidel relaxation. Therefore, the validity of the above

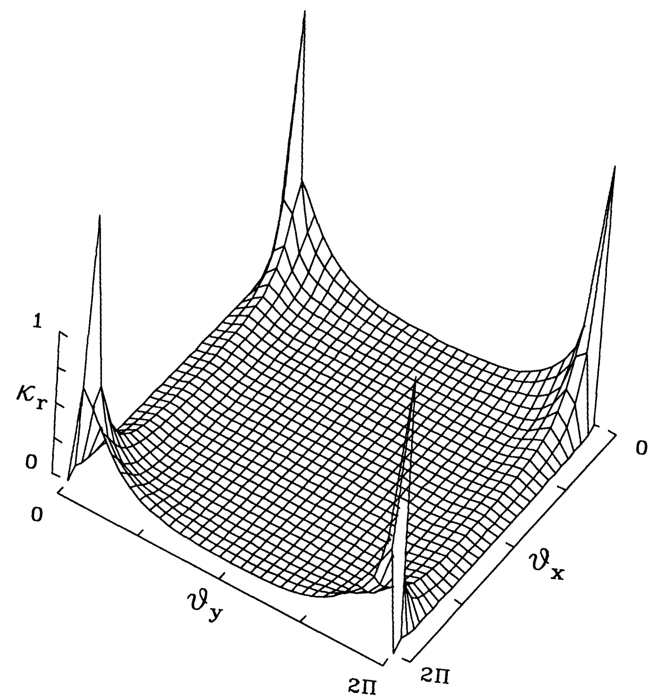

FIG. 2. *As Fig.* 1, *but for van Leer's flux-vector splitting.*

analysis may be questioned, especially for the longer waves. In this section the instability will be investigated by numerical experiments on the system of nonlinear Euler equations (2.1).

For the upwind differencing, van Leer's flux-vector splitting (FVS) [14] is used as an approximate Riemann-solver. This scheme gives rise to matrices $A^{\pm} \equiv df^{\pm}/dw$ and $B^{\pm} \equiv dg^{\pm}/dw$, which are different from those in (2.7). Therefore, the stability properties of this scheme will be different from those predicted in the previous section, but not by too much. Figure 2 shows the amplification factor for FVS, using the same parameters as in Fig. 1.

As a test problem, flow through a straight channel is considered. The grid is square and uniform. There are hard walls on the lower and upper sides. Boundary conditions at the walls are implemented by mirror cells that contain reflected states. Characteristic boundary conditions are used at the inlet and outlet. In principle, overspecification can be used because the Riemann-solver takes care of the appropriate switching between incoming and outgoing characteristics. However, because FVS is not a very good approximate Riemann-solver, the use of characteristic boundary conditions is recommended.

The free-stream values are chosen to be

$$\rho_\infty = 1, \qquad u_\infty = 0.8, \qquad v_\infty = 0, \qquad c_\infty = 1, \tag{3.1}$$

whereas the gas-constant $\gamma = 1.4$. As initial conditions, we take the free-stream values and add random noise with an amplitude of 10^{-5}. The steady state is given by the free-stream values.

TABLE 1

Amplification factors for flux-vector splitting on grids of various sizes, with $u_\infty/c_\infty = 0.8$ and $v_\infty/c_\infty = 0.0$. The result of the Fourier stability analysis is denoted by $\overline{\kappa}_r$. The other values are determined from numerical experiments on the full system of nonlinear Euler equations.

N	$\overline{\kappa}_r$	Observed
16×16	0.594	0.80
32×32	1.853	1.45
64×64	4.096	2.55

Table 1 shows the predicted and observed amplification factors. There is a clear qualitative agreement. Inspection of the difference between the nonconverged solution and the numerical steady state confirms the long-wave instability.

4. Multigrid. The instability of SLGS occurs for the long waves. It is therefore expected that the combination of SLGS and the multigrid technique will provide a stable scheme. The analysis of multigrid convergence for the linearized Euler equations with constant coefficients is presented in detail in [9]. The multigrid convergence factor $\overline{\lambda}_r$ of a given relaxation scheme is estimated by considering two grids, a fine and a coarse. The number of cells on the coarse grid is one-fourth of that on the fine. For the restriction to the coarser grid, simple averaging is used. Piecewise constant interpolation is applied for the prolongation back to the fine grid (cf. [7]). In the analysis, it is assumed that the coarse-grid equations are solved exactly. The combined result of the coarse-grid correction and the relaxation scheme is described by $\overline{\lambda}_r$. This two-level multigrid convergence factor gives a reasonable estimate of the convergence speed when many coarser grids are used.

The result of the so-called two-level analysis is shown in Fig. 3. The instability has disappeared. The overall convergence rate is good, except near the singularities of the (linear) residual. The slow convergence around $v = 0$ occurs when the flow is aligned with the grid over a substantial part of the computational domain. To overcome the problem of strong alignment [2], one might consider a relaxation scheme that consists of a SLGS step with the line in the x-direction, followed by SLGS with the line in the y-direction. This will be called Alternating Direction SLGS. ADSLGS turns out to be stable in a larger region of the $(u/c, v/c)$-plane. However, the instability persists for some parameters and is so severe that it does not disappear in a multigrid scheme.

A scheme that suffers from strong alignment in a similar way as SLGS is damped Symmetric Point Gauss–Seidel (SGS) [9]. It is stable as a single-grid scheme and much cheaper than its undamped line variant, and is therefore to be preferred. If one wants a uniformly good convergence rate, a multigrid scheme that employs damped Alternating Direction Line Jacobi (ADLJ) can be used. The linear two-level analysis predicts a multigrid convergence rate $\overline{\lambda}_r(u/c, v/c) \leq 0.526$ for this scheme. The relaxation operator is described by the product of line relaxation in the y-direction, namely,

$$\hat{G}_1 = I - \hat{H}_1^{-1}\hat{L}^h, \qquad \hat{H}_1 = \hat{L}^h + \frac{1}{h}[A^+(\hat{T}_x^{-1} + 1) - A^-(\hat{T}_x + 1)], \tag{4.1a}$$

and line relaxation in the x-direction:

$$\hat{G}_2 = I - \hat{H}_2^{-1}\hat{L}^h, \qquad \hat{H}_2 = \hat{L}^h + \frac{1}{h}[B^+(\hat{T}_y^{-1} + 1) - B^-(\hat{T}_y + 1)]. \tag{4.1b}$$

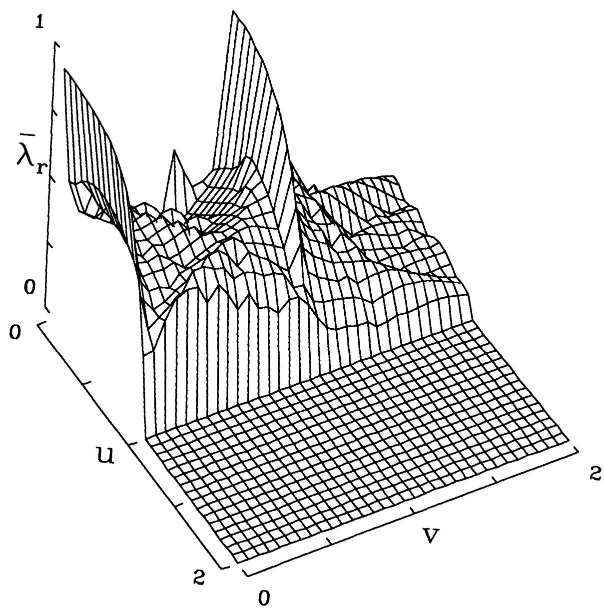

FIG. 3. *Multigrid convergence factor for* SLGS *relaxation as a function of* u *and* v $(c = 1)$. *Each point is computed for a* 64×64 *grid.*

Note that the relaxation operators H_1 and H_2 are obtained by selecting the main-diagonal (in terms of blocks) and two off-diagonals (in one direction) from the residual operator. The damping is obtained by subtracting the two other off-diagonals in the direction perpendicular to the line from the main-diagonal. Figure 4 shows the two-level multigrid convergence rate for damped ADLJ relaxation.

5. Conclusions. SLGS relaxation is unstable if used for the implicit upwind differenced Euler equations. The instability occurs for the long waves and, therefore, must be sensitive to the numerical boundary conditions and the precise form of the spatial discretization. The instability is predicted by linear Fourier analysis, which is not completely appropriate for this relaxation scheme. However, numerical experiments on the nonlinear equations confirm the long-wave instability.

The instability can be suppressed by a multigrid scheme. However, in that case damped Symmetric Point Gauss–Seidel is a better choice, because it is stable as a single-grid scheme and can produce similar multigrid convergence factors at a much lower cost [9]. This scheme, however, does not provide good convergence in cases of strong alignment, the flow being aligned with the grid.

A uniformly good convergence rate can be obtained with damped Alternating Direction Line Jacobi, which has about the same cost as SLGS. The two-level analysis indicates a convergence factor that is at worst 0.562.

The use of SLGS has been recommended for the Navier-Stokes equations in [5]. Numerical experiments in [6] suggest grid-independent convergence rates. Because the

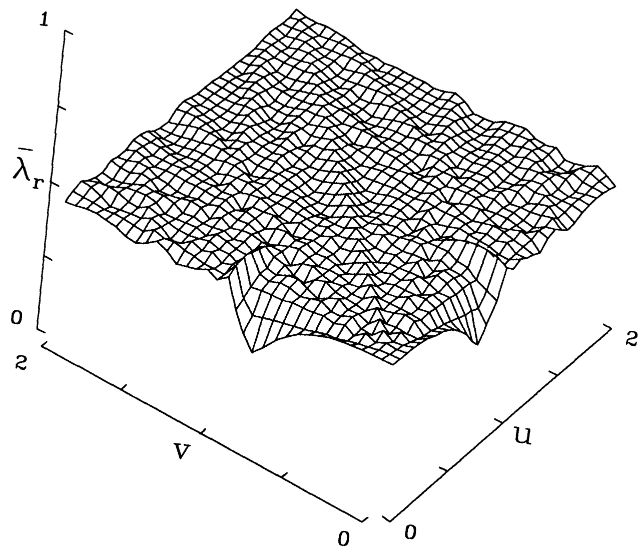

FIG. 4. *Multigrid convergence factor for* ADLJ *relaxation as a function of u and v* ($c = 1$). *Each point is computed for* 64×64 *grid.*

spatial discretization is essentially different in the long-wave regime, due to viscous terms and a different form of flux-splitting, the present analysis does not automatically carry over to this situation.

Finally, it should be noted that the results of two-level analysis tend to be too pessimistic. If one considers a wave perpendicular to a streamline, i.e., $u\theta_x = -v\theta_y$, and concentrates on the long waves (small θ_x and θ_y), the coarse-grid correction operator $\hat{K}$ can be approximated by $\hat{K} \simeq I - (\hat{L}^{2h})^{\dagger}\hat{L}^h$, which has an eigenvalue $\frac{1}{2}$. This value will dominate the results of two-level analysis, as can be seen in Fig. 4. However, the eigenvalue corresponds to a wave for which the exact operator vanishes and, therefore, describes convergence of the truncation error. If one is only interested in convergence to a level where the iteration error is of the order of the truncation error, this value is clearly not important. The reader is referred to [10], [11], [12] for further details and applications.

REFERENCES

[1] R. W. BEAM AND R. F. WARMING, *An implicit finite-difference algorithm for hyperbolic systems in conservation-law form*, J. Comput. Phys., 22 (1976), pp. 87-110.

[2] A. BRANDT, *Guide to multigrid development*, Lecture Notes in Math., 960 (1981), pp. 220-312.

[3] S. R. CHAKRAVARTHY, *Relaxation methods for unfactored implicit upwind schemes*, AIAA paper no. 84-0165 (1984).

[4] J. DOUGLAS AND J. GUNN, *A general formulation of alternating direction methods*, I, Numer. Math., 6 (1964), pp. 87-110.

[5] R. W. MACCORMACK, *Current status of numerical solutions of the Navier-Stokes equations*, AIAA paper no. 85-0032 (1985).

[6] Y. J. MOON, *Grid size dependence on convergence for computation of the Navier-Stokes equations*, AIAA J., 24 (1986), pp. 1705-1706.

[7] W. A. MULDER, *Multigrid relaxation for the Euler equations*, J. Comput. Phys., 60 (1985), pp. 235-252.

[8] ———, *Computation of the quasi-steady gas flow in a spiral galaxy by means of a multigrid method*, Astron. and Astrophys., 156 (1986), pp. 354-380.

[9] ———, *Analysis of a multigrid method for the Euler equations of gas dynamics in two dimensions*, in Multigrid Methods: Theory, Applications, and Supercomputing, S. McCormick, ed., Marcel Dekker, New York, 1988, pp. 467-489.

[10] ———, *A new multigrid approach to convection problems*, J. Comput. Phys., 83 (1989), pp. 303–323.

[11] ———, *Multigrid, alignment, and Euler's equations*, presented at the Fourth Copper Mountain Conference on Multigrid Methods, Copper Mountain, Colorado, April 1989. To be published by SIAM.

[12] ———, *A high resolution Euler solver*, AIAA paper no. 89-1949 (1989).

[13] J. L. THOMAS, B. VAN LEER, AND R. W. WALTERS, *Implicit flux-split schemes for the Euler equations*, AIAA paper no. 85-1680 (1985).

[14] B. VAN LEER, *Flux-vector splitting for the Euler equations*, Lecture Notes in Physics, 170 (1982), pp. 507-512.

[15] B. VAN LEER AND W. A. MULDER, *Relaxation methods for hyperbolic conservation laws*, in Numerical Methods for the Euler Equations of Fluid Dynamics, F. Angrand, A. Dervieux, J. A. Desideri, and R. Glowinski, eds., Society for Industrial and Applied Mathematics, Philadelphia, PA, 1985, pp. 312-333.